Preliminary analysis of a soft storey mechanism after the 2009 L'Aquila earthquake

Gerardo M. Verderame, Flavia De Luca(*),
Paolo Ricci and Gaetano Manfredi

Department of Structural Engineering, DIST, University of Naples Federico II,
Via Claudio, 21, 80125 Naples

(*) **Corresponding author: flavia.deluca@unina.it**

Abstract

Observation of damage caused by the recent Abruzzo earthquake on April 6th 2009 showed how local interaction between infills and RC structures can lead to soft storey mechanisms and brittle collapses. Results of the present case study are based on observed damage caused by the earthquake in the zone of Pettino. Analytical model based on simulated design procedure was built up and time history analyses were employed to verify the causes of the structural collapse, as highlighted by observed damage. This failure mechanism was investigated taking into consideration all components of the ground motion. Nonlinear behavior of brick masonry infills was taken into account and two parametric hypotheses for infill mechanical properties were considered, given the uncertainties that typically characterize these nonstructural elements. Nonlinear modeling of infills was made by a three strut macro-model aimed at considering both local and global interaction between RC frame and infills. Seismic input was characterized by the real signal registered during the mainshock near the case-study structure. Different shear capacity models were considered in the assessment.

Analytical results seem to confirm with good approximation the likely collapse scenario that damage observation highlighted; the lack of proper detailing in the columns made the local interaction between infills and RC columns and the strong vertical component of the ground motion to be the main causes of the brittle failure.

Keywords: L'Aquila earthquake, RC structure, soft storey, infill, interaction, brittle failure

1. Introduction

The majority of reinforced concrete buildings in L'Aquila showed non-structural damage and only a few structural collapses were observed.

Observation of damage on RC structures after L'Aquila event emphasized the importance of taking into account the contribution of nonstructural elements such as infills. Most of the observed damage was localized in infill panels and their stiffness and strength contribution in some cases preserved the RC buildings from structural damage. On the other hand, it is to note that infill irregular distribution in plan and elevation can be addressed as one of the main causes of the structural collapses observed during in-field campaigns, together with obsolete design criteria according to which those buildings were designed [1].

Most of the buildings in the region struck by the earthquake were built between the 1960s and 1990s, when the province of L'Aquila was classified as a medium-low seismic intensity zone. Spectral comparisons between inelastic acceleration of old codes, recent Italian seismic code demand [2] and seismic demand of the earthquake emphasized a lack of global ductility in the existing buildings [1]; in fact, old seismic codes did not consider *performance based design* approach. That is why main criteria for seismic design such as *capacity design* and prescriptions regarding minimum reinforcement requirements, both longitudinal and

transversal, aimed at increasing both the global and the local ductility of structures, were not considered.

According to actual seismic codes, such as the Eurocode 8 [3], specific prescriptions are provided regarding structural detailing and masonry infill issue is also considered: in new design buildings infill walls need to be considered in the modeling if they contribute significantly to the lateral stiffness and resistance of the building. According to Eurocode 8, infills in principle are still considered as nonstructural elements but in any case special provisions should be applied if masonry infills are vulnerable to out-of-plane failures. Out-of-plane failures of infills represent another critical issue that damage observed after L'Aquila earthquake emphasized [4].

Masonry infill role can be even more relevant in existing structures; that is why the analysis of seismic response of existing RC buildings should take into account the presence of infill elements and interaction between these elements and the primary RC structural system.

Effect of infills on the whole structural behavior depends on different factors that are briefly recalled in the following and have been studied in dedicated papers.

Firstly, the evaluated fundamental period of the infilled structure [5] changes significantly if compared to the period of the bare frame model, since the structure is significantly stiffer. Furthermore, infill presence can change regularity characteristics of the structure in plan and in elevation and consequently can affect the mode of vibration of the building. In other studies made after other earthquakes that struck the Mediterranean area it is already emphasized the importance of infill contribution in the evaluation of seismic performances of RC buildings [6].

Secondly, infills are characterized by a brittle behavior and the high contribution in strength they supply to a RC building suddenly decrease for low values of drift [7]. On the other hand, it is worth to note that infill impact on the structural performances of buildings becomes a critical issue when RC primary elements are designed according to obsolete criteria and the structure is characterized by an insufficient global and local ductility. The latter can be observed when seismic performances of contemporary and existing infilled frame structures are compared [8].

Infilled RC building behavior can be significantly different if low or high level of seismic intensity is attained [6].

If infill distribution is irregular in plan or elevation, their contribution introduces a source of irregularity (e.g. *Pilotis effect*) and the possibility to register a soft-storey mechanism is dramatically increased, especially when no capacity design criterion has been employed in the design of the bare frame [6].

Mechanical properties of the infills represent another critical factor that can vary the effect of infills on the performances of the whole structure, since they are considered nonstructural elements and their properties, not systematically checked, can vary significantly [9] because of the local building practice. Regarding this latter issue, it is important to stress the relative weight that infills have respect to the mechanical properties of the bare frame.

Because of all the variables considered (seismic intensity level, old or contemporary design approach, distribution and mechanical properties of the infills) it is tough to say if structural contribution of these "nonstructural" elements increases or decreases the overall seismic capacity of the building.

In this paper one of the few collapsed buildings after L'Aquila earthquake is assumed as case study; the building collapsed as a result of a soft storey mechanism at the first storey. Observed damage points to collapse as a result of a brittle failure mechanism.

Given the likely scenario collapse inferred by observed damage, an analytical model of the building was built up taking into account nonlinear behavior of the infills; local interaction with columns was also considered by means of a three strut macro-model [10,11,12]. Two parametric hypotheses based on Italian code [13] prescriptions were assumed for infill

mechanical properties. Time history analyses were carried out assuming as seismic input the three components of the real registered signals during the mainshock in the vicinity of the case study structures.
The study represents a preliminary approach because of the uncertainties regarding knowledge of the building.
Given the brittle failure highlighted by damage, beside capacity models suggested by codes [14], other shear failure mechanisms not typical for columns [15] were considered.
Numerical results seem to confirm the collapse scenario inferred by damage observation; the lack of proper structural and executive details was addressed as the main cause that made a critical issue the local interaction between columns and infills, other than the strong vertical component registered.

2. Damage Observation

In the following section, geometrical and structural characteristics of the case study building and the damage experienced due to the April 6th event are discussed. Pre- and post-event photographic images [16] and in-situ survey allow the determination of the geometry of the structure. Survey was rapidly carried out due to the severe damage of the building. Moreover, some insights into the possible reasons for the collapse are reported.

2.1 Structure description

The case study structure is part of a group of residential buildings realized during 1980s in Pettino (L'Aquila).
The morphology in plan is irregular, approximately T-shaped. Three storeys and an attic are present; the first storey is used as a store and a garage, the other storeys are used as habitation. The structure is a three-dimensional RC frame, likely designed for both gravity and seismic loads according to the seismic code prescriptions in force at the time of construction. L'Aquila was classified as a category II seismic zone and the design acceleration on stiff soil was equal to 0.07g [17]. Infill distribution is irregular in elevation due to the presence of openings at the first storey.
Figure 1 reports some aerial photographs of the building before the seismic event; some elements are clearly shown: the irregular plan, the number of storeys, the attic storey and the garage openings at the first level.

Figure 1. Pre-event view of case study building, placed in Pettino (L'Aquila) (Virtual Earth)

No architectonic or structural drawing is available. Nevertheless, in-situ survey, together with a metric evaluation of photographic images, allowed defining the building global dimensions, number and length of bays in external frames. In particular, global dimensions in plan are

approximately (25×30) meters while interstorey height is about equal to 3 meters. Similarly, dimensions of structural elements and reinforcement details can be drawn from the empirical observation of failed elements. Columns at the first storey have a (300×500)mm^2 section. Deformed bars are employed as reinforcement; longitudinal reinforcement consists of eight 12 mm diameter bars, symmetrically distributed along the major section dimension, while transverse reinforcement is made by stirrups (diameter equal to 6 mm), 150 mm spaced. Infill panels consist of a double layer of hollow clay brick infills typical of Italian building practice. Thicknesses of external and internal layers are equal, respectively, to 120 and 80 mm.

2.2 Structural damage

Building collapse involved only first storey elements. In Figure 2, moderate cracking in the upper storey infills is shown.

Collapse mechanism is not translational. The position of first storey failed columns suggests that the building collapsed under a torsional mechanism, as simply schematized in Figure 3.

(a) (b)

Figure 2. Building collapse mechanism. Damage along South-East (a) and South-West (b) wings of the building [15]

First storey columns in the most distant frame from the centre of the masses frame (1-2-3) show displacements approximately equal to tens of centimeters in X direction and very small in Y direction; in similar way columns in the perpendicular frame (15-23-31) show displacements of few centimeters in Y direction and very small in X direction. Corner columns are totally separated from the rest of the building. Columns #1 and #22 reported in Figure 3 kept their original position, without showing any plastic rotation; therefore, the actual position of the collapsed building with respect to these elements is evidence of the movement associated to the collapse mechanism that resulted after the failure of the first columns. Due to this collapse movement, the structure, from the second storey on, completely lost its connection with columns #1 and #22.

Collapsed columns #3 and #38 show evident damage; these elements were involved in the rotational collapse movement of the remaining part of the structure and their conditions seem to suggest that the building crashed into them.

Moreover, it should be noted that in both kinds of damaged columns (#1, #22 and #3, #38) the longitudinal reinforcement was torn up from the concrete core of the column, due to the absence of a proper restrain; the absence of transversal reinforcement in beam-column joints, the low diameter of the stirrups in columns and the deficiency in closure detail of these stirrups can be highlighted as contributory causes that favored this specific observed damage.

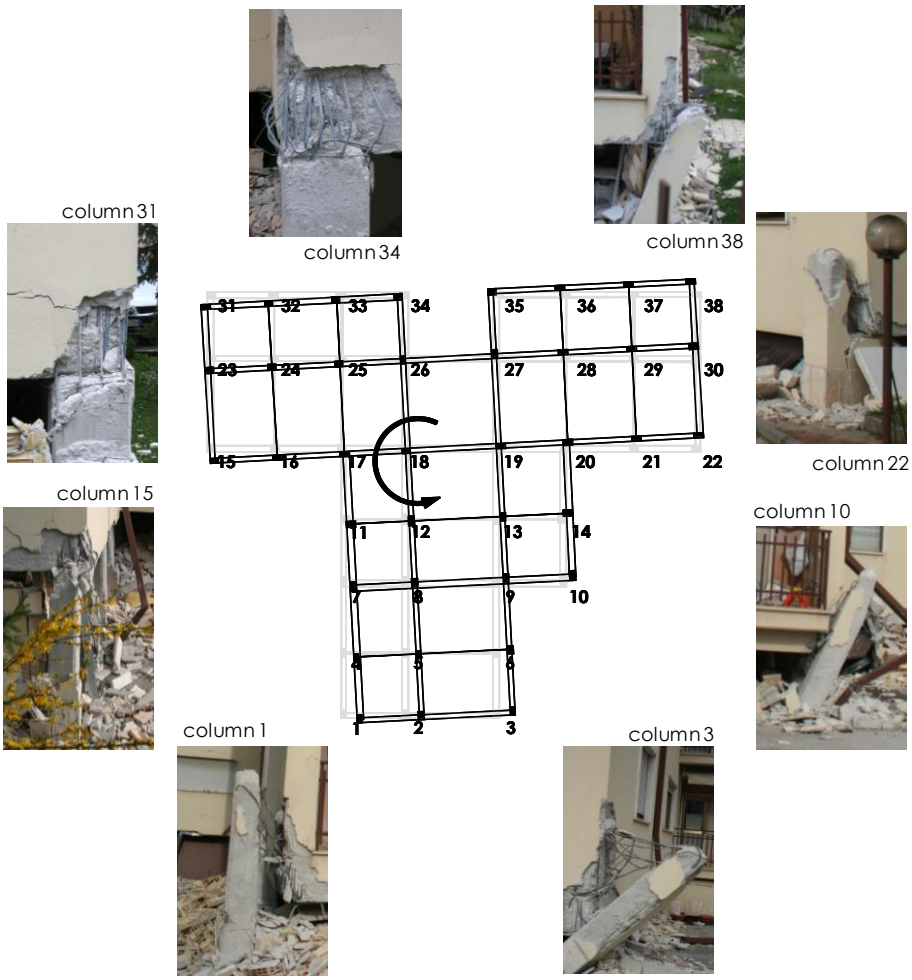

Figure 3. Building collapse: column damage points out a rotational movement

Observation of failed columns shows that no ductile mechanism was developed; loss of contact between column and upper joint is not involved in such a mechanism. Similarly, it can be excluded that geometric non-linear effects such as P-Δ are involved in the collapse. As a matter of fact, this effect is related to high rotational (ductility) demands typical of a *flexure-controlled failure*, which are not shown by failed elements.

Failure is certainly due to a brittle mechanism. Nevertheless, columns' collapse appears to be different from a conventional brittle shear failure, due to a truss mechanism in compressed concrete or in transverse reinforcement. In this case, failure of the elements follows the development of diagonal cracks; moreover, crushed concrete struts and/or yielded transverse reinforcement can be clearly observed after failure. On the contrary, surfaces at the top of failed columns and at the bottom of corresponding joints in the present building are rather smooth (see Figure 4), leading to the hypothesis of a likely frictional failure, located along weak surfaces probably corresponding to a casting separation. Longitudinal bars crossing these surfaces were not restrained by transverse reinforcement, due to the stirrups spacing and to the complete absence of stirrups in beam-column joints. Moreover, transverse reinforcement is closed with 90 degree hooks, therefore not providing an effective anchorage. This kind of failure seems to be confirmed by damage shown in Figure 4b, in a structural element adjacent to a failed infill panel: concrete cover is crushed and longitudinal reinforcement is not restrained. There is no transverse reinforcement in the joint, and the first stirrup at the top of the

column is opened. A clean, deep crack has clearly developed along the interface between the top of the column and the joint.
Upper storeys show no significant damage in structural elements, or in infill walls. The light damage in the upper storeys is clearly due to the rigid post-collapse movement mentioned above.
A likely collapse scenario can be described thanks to the above observation: shear friction failures occurred in the columns characterized by larger seismic loads due to their position in plan (probably #3 and #38). The brittle failure of the first columns and the loss of contact with the above structure at the connection between the top of the first storey columns and beam-column joints produced a rigid collapse movement that made the building crashing into columns #3, #10 and #38 and contemporarily losing any connection with columns on the other side (#1, #15, #31 and #34), which did not show any plastic rotation and stand exactly in the same position they had before the earthquake.
It is to note that the only column in which it is still possible to recognize a shear friction failure is column #31, in the other cases the collapse rigid movement hid the original brittle failure mechanism occurred in the columns, which can be considered the main cause of the whole building collapse according to the likely scenario made up from damage observation.

(a) (b)

Figure 4. Damage highlights not properly treated casting surface (a, b) and absence of stirrups in the joint area (b) [15]

3. Modeling issues

Available information gathered by damage observation, pre-event configuration of the structure and time of construction (between 1980's and 1990's) were used to build up the structural model of the building, aimed at highlight the probable causes of the collapse by means of a numerical approach. Furthermore, it was possible to infer some information from code and building practices of the time [17] and to provide a simulated design procedure [18] of some parts of the structure.
First, configuration and global dimension in plan were determined (Figure 5) using photographic material and a speed in-situ survey in addition to the orientation of external columns, whereas internal columns orientation was determined using building design practices. The distribution of beams in plan is based on the in-situ survey. Figure 5 defines X and Y directions in plan; this coordinate system will be used as a reference in the following section.
Second, in-situ visual survey data allowed determining section dimensions of the external columns and beams at the first storey (see Figure 3); longitudinal and transversal reinforcement of some of the columns at the first storey are also known, as already highlighted at § 2.1. Based on this knowledge, a simulated design procedure was carried out, aimed at determining

dimensions of remaining beams and columns and the longitudinal and transversal reinforcement. To this end, a simplified structural model was employed (shear type model) [18].

Hence, due the number of stories (only three) and the building practices at the time for this kind of structures, all column and beam section dimensions at upper levels were assumed equal to first level section dimensions, partly determined from the in-situ survey and partly from the simulated design procedure.

Column sections were considered equal to (300×500)mm; similarly, beam sections were assumed equal to (300×500)mm. Longitudinal reinforcement in columns at the first storey was composed of eight 12 mm bars placed along the 500 mm sides of the section; transversal reinforcement was composed of 6 mm stirrups 150 mm spaced, and stirrups are closed with a 90 degree hook.

It is worth to note that simulated design of longitudinal and transversal reinforcement was referred only to the first storey columns, since the collapse mechanism did not involve the remaining storeys (section 2.2); this assumption is also confirmed considering other buildings collapsed because of a soft storey mechanism [6], similar to the present case study structure.

Based on Italian design practice, typical unidirectional joint-slabs were assumed, with 400 mm thick hollow bricks and 100 mm thick joists and a 40 mm thick layer of concrete on top. Slab way was assumed along the short directions of the wings and the web of the T-shaped plan (see Figure 5). Dead structural and non-structural loads were evaluated; live load Q_k was given equal to 2 kN/m^2, according to code prescription.

Structural material properties were determined by means of steel and concrete used during the years of construction. Steel properties were evaluated from Italian deformed bars FeB44K; the medium value of the yielding strength f_{ym} was assumed equal to the nominal value of 440 MPa. The minimum value of the concrete strength, according to the code prescriptions in force when the structure was built, was given by f_{ck}=20 MPa. In this case, too, the medium value of the concrete compressive strength f_{cm} was assumed equal to the value f_{ck}=20 MPa.

According to Italian code prescriptions [2] Young modulus of concrete was assumed equal to E_c=27000 MPa. The assumptions made regarding concrete properties will not affect strictly the evaluation of stiffness and modal properties of the structure because the stiffness contribution of infills has a stronger impact on modal properties.

With regards to strength and stiffness infill properties, it was necessary to employ Italian Code [2] provisions, having determined the infill typology from photographic documentation. The structure has double layer brick infills, in the model an equivalent single layer infill was considered 200 (=120+80) mm thick.

Infill properties are characterized by several uncertainties and they affect linear and non-linear behavior of the structure. Therefore, the following two opposing parametric hypotheses regarding infill properties were proposed. The hypotheses assume maximum and minimum values for this typology by Italian Code (despite the possible overstrength due to mortar quality):

- *weak infill* hypothesis is characterized by a value of cracking shear stress (τ_o) equal to 0.30 MPa, and Young modulus (E_w) equal to 3600 MPa considering a ratio of 0.30 between shear modulus G_w and E_w.
- *strong infill* hypothesis is characterized by τ_o equal to 0.40 MPa, and E_w equal to 5600 MPa considering the same ratio of 0.30 between G_w and E_w.

Infill distribution was determined by photographic documentation (see Figure 1).

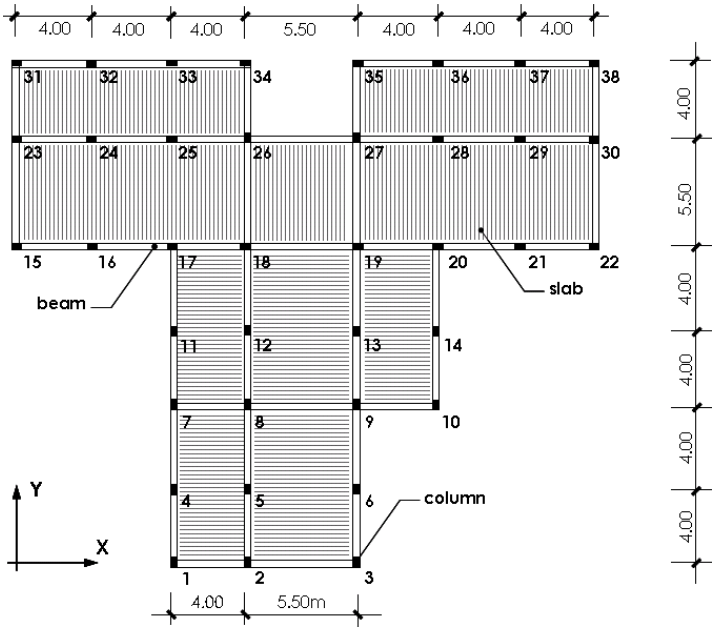

Figure 5. Dimensions in plan, columns orientation

3.1 Linear model

Linear model of the structure was build up according to the two different parametric hypotheses about infill stiffness properties (*weak* and *strong*). Beams and columns were modeled as frame elements, behavior of beam-column joints was assumed to be elastic and a rigid diaphragm constraint was imposed at the floor level.

The infills were modeled by means of a three strut model that will be described in detail in section 3.2.

An elastic shear stiffness (K) is assumed for the infill wall, consistent with the model proposed in [19]:

$$K = \frac{G_w t_w L_w}{h_w} \tag{1}$$

where G_w is the shear modulus of the infills, t_w is the equivalent thickness, L_w and h_w are, respectively, the clear length and the clear height of the infill panel.

The 50% of the whole infill stiffness is assumed to be given by the contribution of the central strut (k_1), similar to other authors [12]:

$$k_1 = 0.50\frac{K}{\cos^2\theta} = 0.50\frac{G_w t_w L_w}{h_w}\frac{1}{\cos^2\theta} \tag{2}$$

while the remaining stiffness, given by the two off-diagonal struts, can be evaluated by the principle of virtual displacements [10]. If an equal axial stiffness (k_2 and k_3) is assumed for the off-diagonal struts, than $k(=k_2=k_3)$ depends on the infill stiffness K and on the axial stiffness of the central strut k_1 according to the following expression:

$$k = (K - k_1\cos^2\theta)/\left[2(1-\alpha)^2\cos^2\theta\right] \tag{3}$$

Infills placed at the attic level, above the third level, were modeled as shell membrane elements, characterizing material with infill stiffness properties. A different model was adopted for these elements because of their low height and their non-rectangular shape, which would make not properly adequate a strut modeling.

According to the two infill properties (*weak* and *strong*), two different linear models were considered and their dynamic properties were evaluated. Modal properties of the structures are summarized in Table 1; for each of the two models, the first mode has participant mass ratio essentially in X direction, showing a torsional shape in X-Y plan; the second mode is translational in Y direction; the third is a torsional mode. Differences between the first period (T) of the structure in the two infill properties hypotheses (*weak* and *strong*) provide an idea on how infill stiffness can influence structure global stiffness showing a difference between period values that is over 15%.

mode	strong infills				weak infills			
	T sec	**UX** [%]	**UY** sec	**RZ** [%]	**T** sec	**UX** [%]	**UY** sec	**RZ** [%]
1	0.16	78	1	0.16	78	1	0.16	78
2	0.14	1	2	0.14	1	2	0.14	1
3	0.12	18	3	0.12	18	3	0.12	18

Table 1. Modal properties of structure models

In Figure 6, as an example, one of the models (*strong infills*) of the structure, made up by a user-friendly interface software [20], is represented; in particular deformed shapes in X-Y plan at the third level of the structure are reported.

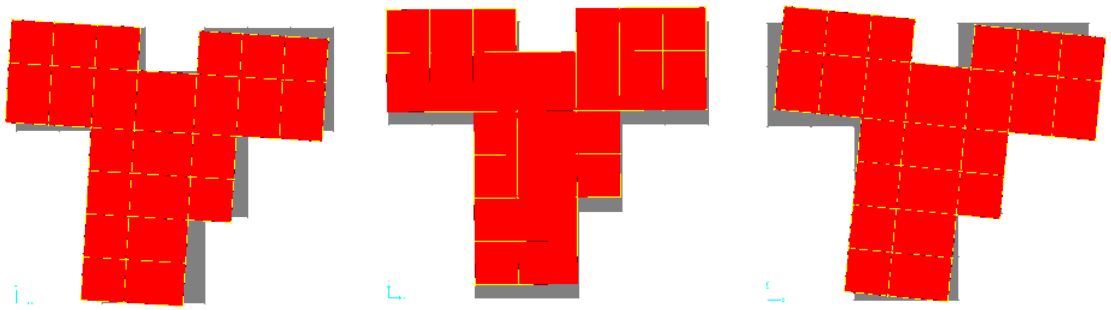

1st mode 2nd mode 3rd mode

Figure 6. Modal deformed shapes in X-Y plan

3.2 Non linear element modeling and capacity models

Modeling of structural and non-structural elements (infills) is based on the in-situ observation of damage suffered by the building, which highlights a brittle failure mode.
Based on the damage survey, the following observations can be carried out:

- damage is only concentrated at the first storey (soft storey mechanism); at upper levels the interstorey displacement demand did not even lead to the cracking of infill panels;
- no evidence of plastic rotation demand (that is, ductile failure mechanism) is present in columns at first storey, involved in the collapse mechanism;
- some columns, probably first causing the global collapse, point out the evidence of a brittle failure mechanism (shear failure);
- infills at first storey are completely failed or heavily damaged.

Hence, consistent with these considerations, the following modeling assumptions are made for the structural elements:

- beams and columns are modeled as elastic. Nevertheless, the possible overcoming of the yield limit and of the strength capacity for brittle failure mechanisms is verified through adequate capacity models, by means of a comparison carried out *a posteriori*

between the strength demand obtained from the analysis and the strength demand given by the above mentioned capacity models;

- infills are represented by a non-linear three strut model. A non-linear modeling is needed not because of the damage suffered by the infills. Moreover, a three strut model, unlike a single strut model, allows to take into account the local interaction phenomena between the infill panel and the surrounding RC elements.

Non linear infill modeling

Modeling of infills is aimed at analyzing the local interaction effects between the infill panel and the surrounding RC elements. To this end, two different modeling approaches can be adopted: the infill panel can be represented by non-linear shell elements and the panel-element interface by spring elements [21]; the infill panel can be represented by strut macro-models [12]. Former models are characterized by a higher detail level, nevertheless latter models are widely spread, also due to the lower computational effort needed.

In the present study a strut macro-model is adopted for infill panels. In particular, six struts, carrying load only in compression, are adopted to represent each panel. As a matter of fact, even if the single strut model is quite easy to be implemented, it is not able to represent the actual distribution of bending moments and of shear forces in frame members due to the local interaction with the infill panel, as already pointed out by many authors [22,23]. Only the use of two more struts, right placed, besides the central one, allows to account for this interaction [10,11,12].

The central strut lies along the diagonal of the bay frame, from one corner to the opposite. The position of two remaining struts depends on the extension of the contact area along which the load transfer between the infill panel and the RC elements takes place, see Figure 7a. The amount of this area depends on the stiffness and on the deflected shape of the frame members. The length of the contact area, according to several authors [10,11], can be expressed by the following relationship:

$$z = \frac{\pi}{2 \cdot \lambda_h} \cdot h_w = \alpha_c \cdot h_w \tag{4}$$

with

$$\lambda_h = h_w \cdot \sqrt[4]{\frac{E_w \cdot t_w \cdot \mathrm{sen}(2\theta)}{4 \cdot E_c \cdot I_c \cdot h_w}} \tag{5}$$

where h_w is the infill height, L_w is the infill length in plan, t_w and E_w are the thickness and Young modulus of the infill, I_c and E_c represent RC columns' inertia and Young modulus, while tgθ is ratio between h_w and L_w. Ina similar way it is possible to evaluate the extension of the contact area between the infill panel and the adjacent beam; nevertheless, for the sake of simplicity it is assumed to be $\alpha_b = \alpha_c$ [24]. Hence, the three struts are parallel to each other. The off-diagonal struts are placed at a distance equal to (z/2) from the beam-column intersection.

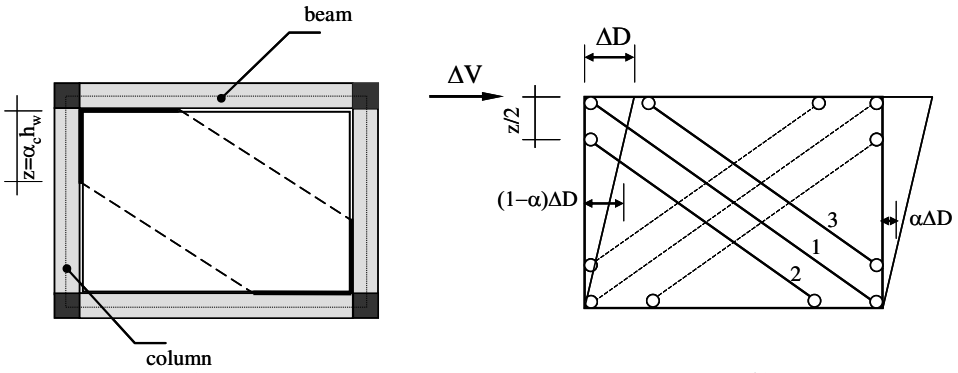

Figure 7. Three strut macro-model adopted for infill panels

The adopted three-strut model has to reproduce the force-displacement response of the infill panel. To determine this curve, the model proposed in [19] is adopted: the envelope curve is given by four different segments as shown in Figure 8a: the initial shear behavior of the uncracked panel; the equivalent strut behavior of the cracked panel; the instability of the panel over its maximum strength; the final stage of the panel when the failure is achieved and the residual strength remains constant.

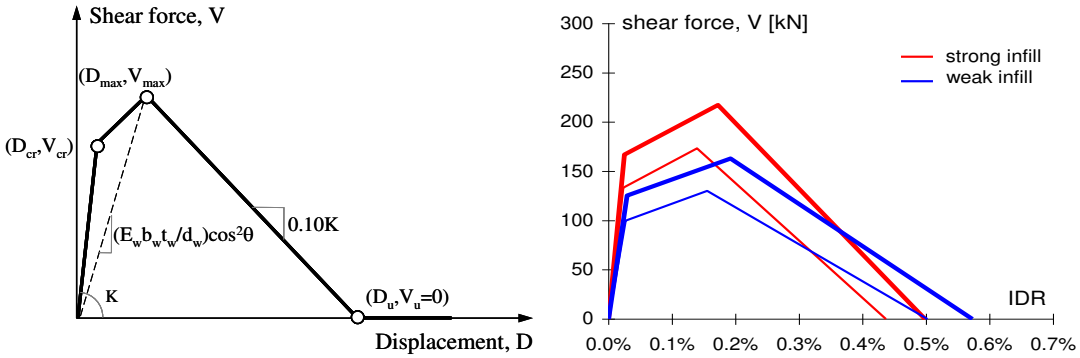

Figure 8. Shear force-displacement envelope proposed by [19] (a), specific shear force-IDR envelopes in structural model (b)

The main parameters of the model are:

(i) initial stiffness of the uncracked wall, K, obtained as

$$K = G_w t_w L_w / h_w \tag{6}$$

(ii) secant stiffness, corresponding to the maximum infill strength, given by the axial stiffness of an equivalent strut:

$$\frac{E_w b_w t_w}{d_w} \cos^2 \theta \tag{7}$$

where t_w and E_w are the thickness and Young modulus of the infill, tgθ is ratio between h_w and L_w, d_w is the diagonal length of the infill panel ($d_w = \sqrt{h_w^2 + L_w^2}$) while b_w was evaluated according to Mainstone's formula [25]:

$$b_w = \left[0.175 \cdot \left(\lambda_h \cdot h_w \right)^{0.4} \right] \cdot d_w \tag{8}$$

(iii) cracking load, V_{cr}, that can be computed as:

$$V_{cr} = \tau_o \cdot t_w \cdot L_w \tag{9}$$

where τ_o is the cracking shear stress;

(iv) maximum load given by:

$$V_{max} = 1.30 \cdot V_{cr} \tag{10}$$

It is assumed, consistent with other authors [10], that the central strut carries 50% of the whole load carried by the infill. Therefore, the axial load-axial displacement relationship of the central strut can be evaluated by the components of the lateral load-displacement relationship of the infill panel along the strut axis:

$$\Delta F_1 = 0.50 \frac{\Delta V}{\cos\theta} \tag{11}$$

$$\Delta \delta_1 = \Delta D \cos\theta \tag{12}$$

$$k_1 = \frac{\Delta F_1}{\Delta \delta_1} = 0.50 \frac{\Delta V}{\Delta D} \frac{1}{\cos^2\theta} = 0.50 \frac{K}{\cos^2\theta} \tag{13}$$

where ΔF_1 and $\Delta \delta_1$ are the incremental axial load and the incremental axial displacement, respectively, corresponding to 50% of the incremental lateral force ΔV and of the incremental lateral displacement ΔD of the infill panel, while k_1 is the axial stiffness of the central strut and K is the lateral stiffness of the infill panel.

Axial load-axial displacement relationships for off-diagonal struts are derived by assuming that the off-diagonal struts complement the central strut in obtaining a behavior equivalent to that of an infill panel.

The equilibrium equation between the shear in the infill panel and the forces in the struts is obtained using the principle of virtual displacements and assuming the same virtual displacement field as shown in Figure 7b. The incremental shear in the infill panel ΔV is expressed as a function of the incremental forces in the three struts.

$$\Delta V = \left[k_1 \Delta \delta_1 + k(1-\alpha)(\Delta \delta_2 + \Delta \delta_3)\right] \cos\theta \tag{14}$$

where k is the axial stiffness of off-diagonal struts, evaluated by means of equation (3), while $\Delta \delta_2$ and $\Delta \delta_3$ are the incremental displacements corresponding to the incremental lateral displacement ΔD of the infill panel.

From this equation, the incremental axial forces in the struts can be obtained as:

$$\Delta F_1 = k_1 \Delta \delta_1 = k_1 \Delta D \cos\theta \tag{15}$$

$$\Delta F_2 = k(1-\alpha)\Delta \delta_2 = k(1-\alpha)^2 \Delta D \cos\theta \tag{16}$$

$$\Delta F_3 = k(1-\alpha)\Delta \delta_3 = k(1-\alpha)^2 \Delta D \cos\theta \tag{17}$$

where ΔF_1, ΔF_2, and ΔF_3 are the incremental forces in the central, upper, and lower struts, respectively.

Equation (3) is used to calculate the stiffness of the off-diagonal struts, and Eqs. (16) and (17) the incremental force in the off-diagonal struts, consistent with the load-displacement relationship assumed for the infill panel.

Finally, a Takeda hysteretic rule was assumed; it is worth noting that considering infill envelope characterized by very low IDR values as shown in Figure 8b, the hysteretic rule chosen does not strictly influence results.

Bending capacity model

Bending behavior was evaluated *a posteriori* on analysis results, no plastic hinges were introduced in the model. In particular, it has to be verified if the bending demand exceeds or not the yield limit of the section. Of course, the overcoming of this limit would not correspond to a ductile failure of the member, but it would mean that the basic hypotheses of the linear model were not satisfied.

This verification is carried out only on columns and not on beams, since the collapse mechanism involved only columns at first storey. To this end, for each section the axial load-yielding moment relationship is evaluated and the yielding moment is evaluated step-by-step, depending on the axial load, and compared with the moment demand.

The biaxial bending interaction between M_x and M_y is not taken into account.

Shear capacity model

Shear behavior was evaluated *a posteriori* on analysis results, no shear plastic hinges were introduced in the model. Different models of shear capacity were evaluated considering the likely brittle failure shown by damage observation.

The capacity model employed is the approach suggested by Eurocode 8 part 3 [14] that employs a different formulation as long as the shear span ratio of the column is above or below 2.

If the shear span ratio (L_V/h) is higher than 2, shear strength is controlled by the stirrups. Shear strength is given by three contributions, respectively related to: axial load (only in compression), concrete resistance mechanisms and transversal reinforcement. Moreover, shear strength decreases as the displacement (that is, the ductility demand) increases. In particular, the cyclic shear resistance, V_R, decreases with the plastic part of ductility demand $\mu_{\Delta pl}$, expressed in terms of ductility factor $\mu_{\Delta pl} = \mu_\Delta - 1$ according to equation (18).

$$V_{R1} = \frac{1}{\gamma_{el}}\left[\begin{array}{l}\frac{h-x}{2L_V}\min(N;0.55A_c f_c)+ \\ (1-0.05(5;\mu_{\Delta pl}))\cdot\left(0.16\max(0.5;100\rho_{tot})(1-0.16\min(5;\frac{L_V}{h}))A_c\sqrt{f_c}+V_w\right)\end{array}\right] \quad (18)$$

where γ_{el} is equal to 1,15 for primary seismic elements and 1,0 for secondary seismic elements, h is the depth of cross-section; x is the compression zone depth; N is the compressive axial force; L_V =M/V is the ratio moment/shear at the end section, Ac is the cross-section area, taken as being equal to (b_wd) for a cross-section with a rectangular web of width (thickness) b_w and structural depth d; f_c is the concrete compressive strength; ρ_{tot} is the total longitudinal reinforcement ratio, V_w is the contribution of transverse reinforcement to shear resistance, taken as being equal to (for cross-sections with rectangular web of width b_w):

$$V_w = \rho_w \cdot b_w \cdot z \cdot f_{yw} \quad (19)$$

where ρ_w is the transverse reinforcement ratio; z is the length of the internal lever arm and f_{yw} is the yield stress of the transverse reinforcement.

Based on the shear capacity model proposed in EC8, it is possible to evaluate shear failure both in elastic (brittle failure, $\mu_{\Delta pl} = 0$) and in inelastic field (limited ductility failure, $\mu_{\Delta pl} > 0$). In our study, the shear capacity is calculated assuming $\mu_{\Delta pl} = 0$, consistent with the elastic modeling adopted for RC elements (beams and columns).

If the shear span ratio (L_V/h) was less or equal than 2, shear strength is controlled by web crushing along the diagonal of the column, which under cyclic loading may be calculated from the expression:

$$V_{R1} = \frac{4}{7}\left(1-0.02\min\left(5,\mu_{\Delta}^{pl}\right)\right)\left(1+1.35\frac{N}{A_c f'_c}\right)\left(1+0.45\cdot 100\rho_{tot}\right)\sqrt{\min\left(f'_c,40\right)}b_w z * \sin 2\theta \qquad (20)$$

Sliding shear capacity model

On the whole, shear capacity is evaluated only according to a strut model, but it is possible that shear stresses may cause a sliding type of failure along a well-defined plane. Because of external tension, shrinkage, neither treated nor checked casting surface or accidental causes, a crack may form along such a plane even before shear failure occurs [26]. The term *interface shear transfer* is used to designate this mechanism, and possible formulations according to shear friction theory are discussed subsequently.

This kind of shear failure is generally not considered in columns because of the presence of axial force N and the presence of vertical reinforcement well distributed around the periphery of element section, giving more reliance to dowel resistance against sliding of vertical bars [27].

The mechanism of interface shear is different in initially uncracked and initially cracked concrete. In initially uncracked surfaces, the resistant mechanism is characterized by adhesion V_a and friction V_f. When the crack is formed, adhesion contribution is not present anymore but a friction contribution due to clamping action ($V_{f,c}$) is added to the friction contribution due to axial force ($V_{f,N}$) and a new additional contribution due to dowel action (V_d) can develop:

$$V_R = V_{f,N} + V_{f,c} + V_d \qquad (21)$$

Shear friction theory in its original version [28] is based on the determination of clamping action due to yielding stress in reinforcement that produces a compression stress on two sides of the crack. As a result of the interlocking at the interface, the sliding movement leads to a vertical movement perpendicular to the crack; as a consequence, longitudinal reinforcement across the crack surface yields in tension. This theory is based on the following hypotheses: reinforcement should be properly anchored on both sides of the crack, sufficiently to develop yield in steel; whereas concrete must be well confined by stirrups. Therefore, consistent with the original formulation proposed by Birkeland and Birkeland [28] and adopted by international codes [14, 29], the contribution due to clamping action is given by:

$$V_{f,c} = \mu \cdot A_{sl} \cdot f_y \qquad (22)$$

in which A_{sl} is the area of shear-friction reinforcement, f_y is the yield strength of reinforcement and μ is the coefficient of friction. This coefficient depends on the treatment of the sliding surface. Obviously, due to the frictional nature of the resistance mechanism, an increase in the external axial load (that is, in the compression state on the interface area) leads to an increase in the shear strength $V_{f,N}$.

Experimental studies [30] demonstrate that shear friction theory gives a conservative estimate of the shear transfer strength of initially cracked concrete and that dowel action assumes an important role in this particular situation.

The contribution of dowel action is due to the shear displacement subjected by reinforcement across the section. In European [14] and Italian [2] codes this contribution is expressed as:

$$V_d = 0.25 \cdot A_{sl} \cdot f_y \quad (23)$$

Hence, interface shear strength is given by:

$$V_{R2} = \mu \cdot (A_{sl} \cdot f_y + N) + 0.25 \cdot A_{sl} \cdot f_y \quad (24)$$

Friction coefficient μ depends on the treatment of the sliding surface. International code prescriptions in relation to this coefficient are quite different; ACI proposes to assume μ equal to 1.40, 1.00 and 0.60 for monolithic concrete, intentionally roughed surfaces and untreated surfaces respectively, while European codes [14,2] adopt values equal to 0.60 for smooth interfaces and to 0.70 for rough interfaces.

In the case study structure the potential sliding surface corresponds to the casting separation between the top of the column and the beam-column joint, see Figure 4b. In authors' opinion, this surface highlights a poor treatment, similarly to what can be observed in other buildings in Pettino [16]. Therefore, the friction coefficient is given equal to 0.60, as proposed by ACI for untreated surfaces.

Moreover, the value of clamping action contribution directly depends on the amount of an additional reinforcement area A_{sl} [29], which has to be effectively anchored in order to allow the development of a yield stress. In the case study structure such a proper anchorage detail was not present, or failed during the seismic event, see Figure 4; concrete cover crushed in all beam-column joints, thus limiting or even completely removing the upper anchorage of longitudinal reinforcement in columns. Hence, the contribution due to clamping action will not be taken into account in shear strength assessment.

Dowel action mechanism is directly linked to the amount of longitudinal reinforcement in columns. Moreover this reinforcement has to effectively resist a sliding shear movement. If longitudinal bars are placed in the opposite faces of the transverse section, as in the present case study building, this effectiveness depends on the restraining action on longitudinal bars given by transversal reinforcement near the sliding section. Specifically, stirrups placed in beam-column joint and placed at the top of the column. Transversal reinforcement has a low diameter and is closed with 90 degree hooks. Moreover, in corner columns, due to the absence of stirrups in joint area (see Figure 4b); only the restraining action of external concrete cover on longitudinal bars could permit the development of a dowel action mechanism. Therefore, the crushing of concrete cover previously discussed, strongly limits this contribution. In the following section, shear strength will be evaluated both with and without the dowel action contribution (V_{R2}).

Sliding shear behavior was evaluated *a posteriori* on analysis results, no sliding shear plastic hinges were introduced in the model.

4. Nonlinear dynamic analyses

Modeling issues and structural model described in section 3 allow pursuing nonlinear dynamic analyses with the two structural models characterized by the two infill parametric hypotheses (*weak* and *strong*).

Section 4.1 provides information about the L'Aquila event (2009) and input selected for the analyses. The results are presented in section 4.2.

4.1 Earthquake characteristics and seismic input choice

L'Aquila earthquake's mainshock, magnitude (Mw) of 6.8 was characterized by a normal fault mechanism (*dip-slip*). Epicentre coordinates were equal to 42.34 latitude and 13.35 longitude, whereas ipocentre depth was equal to 11.8 km [31]. The case study structure was very close to the epicentre. Three accelerometric stations, whose epicentral distances were less than 6 km,

registered the mainshock event, those stations where chosen also because of the vicinity to the case study structures. In Table 2, station ID and geographic coordinates of each of the stations are reported. Table 2 reports record identifiers (ID), these ID later will be used to identify each accelerogram employed as input for analyses. Figure 9 shows the map of the site in which stations, the epicentre and the case study structure were reported. As it is possible to recognize from the map the closest station to the case study structure (42.376 lat. and 13.354 long.) was AQV (GX066 record), and AQG (CU104) and AQA (FA030) are approximately at the same distance from the structure. Since the principal aim of this study is to find the main causes of the soft storey mechanism showed by the structure during the L'Aquila earthquake mainshock, the three records reported in Table 2 were assumed as input. Horizontal components of the chosen records were rotated considering building orientation in plan and orientation of each component registered to simulate as close as possible the effect of the real shaking on the structure. Each signal was filtered and corrected [32].

Station ID	Record ID	Latitude	Longitude
AQV	GX066	42.377	13.344
AQG	CU104	42.373	13.337
AQA	FA030	42.376	13.339

Table 2. Station IDs and their localization

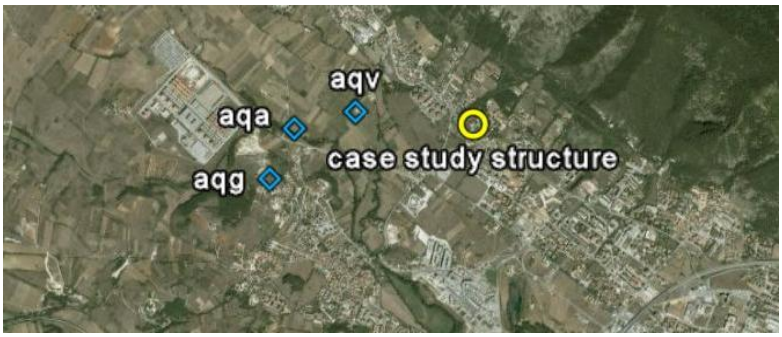

Figure 9. Map of the site, stations, epicentre and case study structure (Google Earth)

The selection procedure adopted in this paper is different from the standard input selection procedure suggested by international codes and literature [33], on the other hand it represents a key tool in providing realistic response for the analyses presented herein.
Elastic spectra of the input signal selected are provided in Figure 10 and compared with code elastic spectra. Elastic spectra of the horizontal components, rotated according to the axes previously assumed in Figure 5, are provided in Figure 10(a). Elastic spectra of the vertical components are provided in Figure 10(b).
In Figure 10, horizontal and vertical Italian code spectra [34] are reported respectively for two different limit states (near collapse SLC and life safety SLV) and for geographic coordinates of the case study structure (42.376 lat and 13.354 long). Different soil type spectra are considered, since it was not possible to determine specific soil type for the site. The accelerometric station closer to the structure (AQV) was characterized by B soil type [31]. According to the code, the vertical component elastic spectra do not present any difference because of soil type.
Considering linear dynamic properties of each model (fundamental period) it is possible to predict roughly the expected response to each single record. For example horizontal components of the closest registered signal (GX066) in period range between 0.2 seconds and 0.25 seconds have spectral ordinates greatly higher than the horizontal components of the other two signals and it has the maximum vertical component in a wide range of periods. It is worth

to note that other dedicated studies highlighted near source effect in the signals considered herein [35].

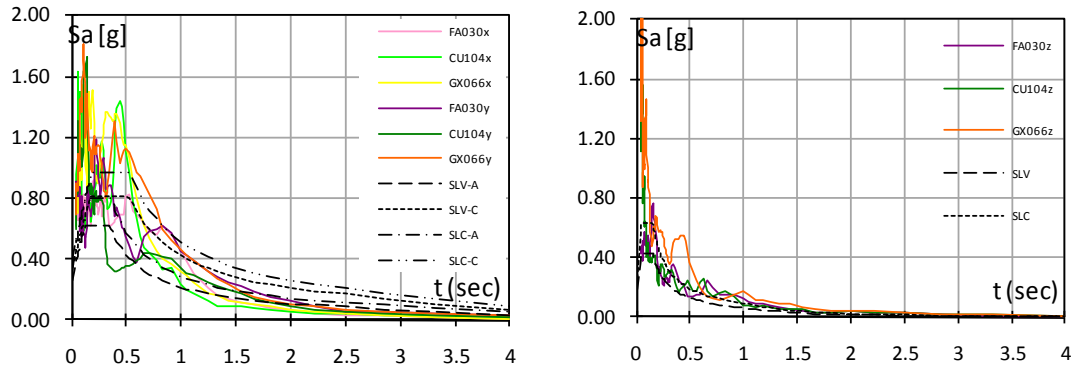

(a) (b)

Figure 10. Elastic spectra for horizontal (a) and vertical (b) components of the record selected compared with target Italian code spectra for the site

4.2 Results and discussion

Results of nonlinear dynamic analyses are presented in this section. For the sake of brevity only the alignment assumed to be more representative of the behavior of the building is presented herein. In particular, the attention is focused on corner columns since, as highlighted in Figure 3, they were particularly damaged.

Moreover, the lower axial load due to gravity loads on these columns, compared to remaining columns, leads to lower strength for flexure, shear and sliding shear mechanisms, given equal the section and reinforcement (both longitudinal and transversal) characteristics.

Furthermore, the higher distance from the centre of masses leads to higher seismic demand, both in terms of forces and displacement, compared to other columns, due to the torsional component of the plan deformation, similarly to what happens for the first modal shape (see Figure 6). Finally, the presence of adjacent infill panels increases the shear demand on these columns, due to local interaction effects.

Therefore, in the following the only results for column #3 at first storey are presented in Figure 11 and discussed. In particular, for the three considered accelerograms, the demand at the top of the column is considered, since, based on analysis results, it is higher than the demand at the bottom.

It is verified (i) if the yield limit is overcome and (ii) if a brittle failure due to shear or to sliding shear occurs. Interaction between axial load and bending moment or shear plays a relevant role for both verifications. To this end, it is sufficient to analyze the first three seconds of the analysis results.

After about 1.50 sec a severe variation in axial load is observed, compared to the gravity load value of 200 kN, up to 100% in compression and 150% in tension. Similarly, bending moment and shear increase too, compared to the almost null values due to gravity loads, but only with a positive or negative sign, respectively.

The high variation in the axial load demand, in particular the variation leading to a compression decrease, contributes to the overcoming of the yield limit after 2.50 sec, for the three considered signals, as highlighted by the evolution of the ratio (M / M_y). As a matter of fact, the high decrease in axial load demand, compared with the gravity load demand, leads to a decrease in the yielding moment M_y, which finally equals the increasing moment demand

M. After that, the results reported in Figure 11 are affected by the fact that the basic hypothesis standing behind the linear behavior of RC elements is not attended anymore. Nevertheless, the overcoming of the yield limit has not to be considered as a ductile failure.

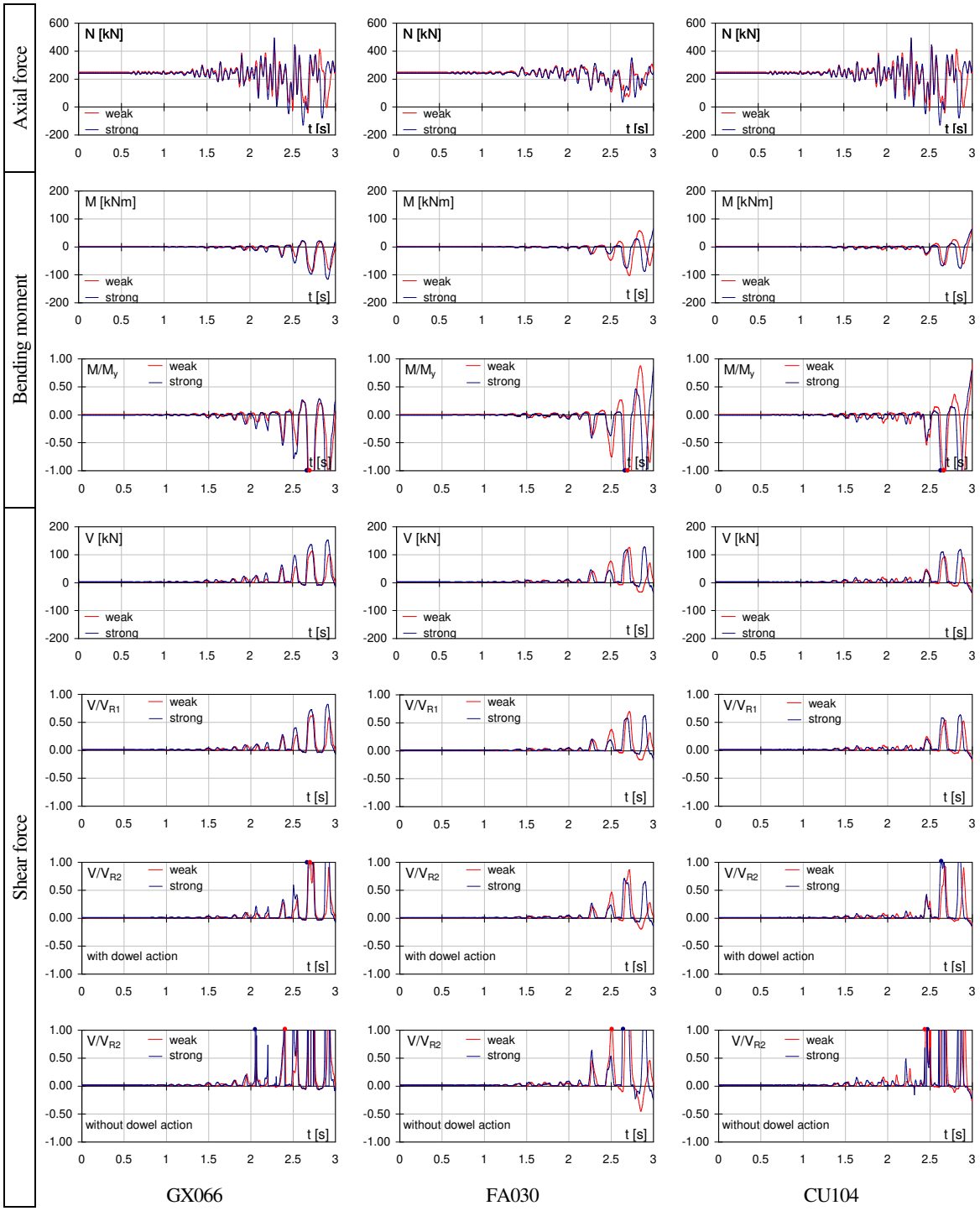

Figure 11. Analysis results for the top of column 3 (axial force, bending moment, shear force demands and demand over capacity ratios)

The increase in shear demand is also coupled with the decrease in axial load demand, nevertheless no shear failure takes place, at least during the first three seconds. In fact, the shear

strength is made up of three contributions (see eq. 18), therefore it is not highly influenced by the variation in axial load.
On the contrary, the sliding shear strength highly depends on the axial load. If the sliding shear strength is considered as given by axial load and dowel action contribution, the sliding shear failure takes place, also in this case, almost at the same time of the section yielding. Only the FA030 accelerogram does not lead to a sliding shear failure during the first three seconds. Moreover, failure occurs for a shear demand about equal to 100 kN, which is given by the local interaction with the adjacent infill panel.
If the dowel action is not considered (section 3.2), the sliding shear strength is proportional to the axial load. The failure occurs before than the previous case, when the dowel action mechanism is considered. This is true for all of the three signals, but above all for the GX066 signal, registered in the closest accelerometric station to the building (about 900 meters), which is probably the most representative one. Moreover, for this signal the vertical component is much severe than for the other signals, see Figure 10b.
Nevertheless, it is worth to note that the shear demand leading to the failure, in this case, is quite low, even less than 50 kN, thus confirming a low value of the load given by the interaction with the adjacent infill panel.
Infill mechanical characteristics (*weak* or *strong*) do not seem to influence strictly the outcome of the verifications.
At the bottom of column #3 the shear and bending moment demand is quite similar to the top of the column. In fact, the maximum values of demand are due, also in this case, to the local interaction with the adjacent infill, through the lower off-diagonal strut, (see Figure 7), even if for an opposite sign of the interstorey displacement. Therefore, from a theoretical standpoint, it is likely to foresee a similar outcome of the verifications: sliding shear failure, section yielding and absence of shear failure.
These considerations are confirmed by graphs reported in Figure 12, for GX066 signal.
Nevertheless, the sliding shear failure, unlike the top of the column, takes place only if dowel action contribution is not considered.
It is to be noted that the hypothesis of absence of dowel action contribution is likely for the top of the column, due to the absence of stirrups in the beam-column joint and to the crushing of the concrete cover (see section 3.2), while it is very conservative for the bottom of the column, because of the restrain action given by the foundation element.
Therefore, the verifications are carried out considering the possible presence or not of the dowel action contribution for the top of the column, and considering only the presence of this contribution for the bottom.
If column #3 is considered as representative of the behavior of corner columns, it is possible to state that the mode of failure is certainly brittle; in particular it takes place due to a sliding shear mechanism at the top of the column, which has a lower strength compared to the bottom. These results seem to be confirmed by the damage observed during the in-situ survey (see Figure 3).

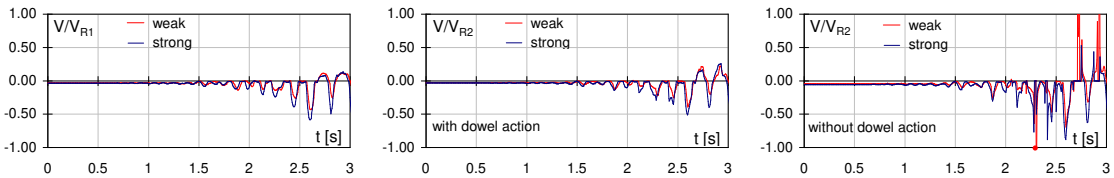

Figure 12. Analysis results for the bottom of column 3 (shear demand over capacity ratios)

Finally, due to the brittle mode of failure, the interstorey displacement demand at the different levels is quite low, following a deformed shape similar to the first modal shape (see Figure 13), and in infills the only cracking displacement is overcome and the maximum strength is not attained.
In particular, referring to column #3, when the sliding shear failure takes place at the top of the column, without considering dowel action, the interstorey drift ratio (IDR) is equal to 0.01% and the adjacent infill is still in elastic field (no cracking is attained), while if the dowel action is considered the IDR value corresponding to failure is 0.1% and the adjacent infill is cracked.
The deformed shape after failure cannot be determined, since no shear hinge is included in the numerical model.

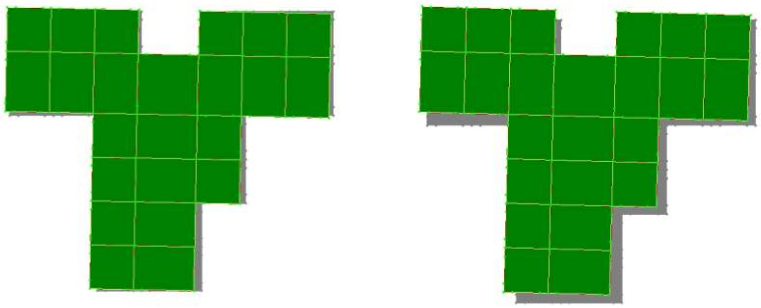

(a) (b)

Figure 13. Plan deformed shape corresponding to the sliding shear failure, (a) without and (b) with dowel action contribution

5. Conclusions

A case study structure that collapsed because of a soft storey mechanism during the 2009 L'Aquila earthquake was studied in this paper.
Photographic documentation and *in situ* survey were used to detect probable failure causes and to collect information regarding the structure.
Damage observation highlights some critical issues that can help to infer the main causes of the collapse. Columns do not show plastic rotation due to a ductile failure mechanism. The way of collapse is clearly brittle, probably caused by a shear friction mechanism, since the failure surface is located along the casting separation between the upper end of columns and the beam-column joints.
A simulated design procedure was employed to attain further knowledge of the structure.
Hence, consistent with the observed failure mode, beams and columns are modeled as elastic. Nevertheless, the possible overcoming of the yield limit and of the strength capacity for brittle failure mechanisms is verified by means of a comparison carried out *a posteriori* between the demand obtained from the analysis and the strength given by adequate capacity models. In particular, bending and shear capacity models were defined according to EC8 prescriptions. Moreover, based on damage observation, a shear friction failure is also considered. The capacity model is defined according to shear friction theory, considering structural details and constructive deficiencies.
Presence of brick masonry infills and their distribution in plan and in elevation were considered in the model. Infill behavior is represented by a non-linear three strut model, which allows taking into account the local interaction phenomena between the infill panel and the surrounding RC elements. Two parametric hypotheses were developed regarding infill mechanical properties.

Seismic input was selected considering the effective registrations of the earthquake; vertical component of the signals was taken into account in the analysis.
Numerical results confirmed the probable cause of failure indicated by damage observation. Analysis demonstrated that the approximation of linear modeling of RC members did not affect the results as soon as the first element failure occurs (localized in the first few seconds of the signals).
The main conclusions drawn from numerical results can be summarized as follows:

- local interaction between infills and RC columns led to an increase in shear demand;
- axial force variation in RC columns, due to vertical component of the earthquake, produced changes in shear capacities more relevant for friction mechanism;
- no shear failure controlled by stirrups or by web crushing occurred;
- the most probable cause of the structural collapse can be addressed to a shear friction failure essentially determined by inadequate transversal reinforcement and improper treatment of casting surface.

The case study presents some peculiar details and results but it does not necessarily represent a common practice or weaknesses in L'Aquila building stock. However, it can help to focus on issues that play an important role when basic seismic design practice is not employed, as it was observed in many other cases documented during in field campaigns.

REFERENCES

1. Ricci P., De Luca F., Verderame G.M. 6th April 2009 L'Aquila earthquake, Italy - Reinforced concrete building performance. *Bulletin of Earthquake Engineering* 2009 (submitted for publication)
2. CS.LL.PP; DM 14 Gennaio 2008: Norme tecniche per le costruzioni. Gazzetta Ufficiale della Repubblica Italiana, 29.
3. Comitè Europèen de Normalisation (2003). Eurocode8, Design of Structures for earthquake resistance – Part1: General rules, seismic actions and rules for buildings. EN 1998-1, CEN, Brussels.
4. Dolce M., Manfredi G. (2009). Research Needs in Earthquake Engineering Highlighted by the 2009 L'Aquila Earthquake, The State of Earthquake Engineering Research in Italy: the ReLUIS-DPC 2005-2008 Project. Editors: Gaetano Manfredi and Mauro Dolce
5. Ricci P., Verderame G.M., Manfredi G. Analytical investigation of elastic period of infilled RC buildings, Engineering Structures 2010 (under review)
6. Dolšek M, Fajfar P. Soft storey effects in uniformly infilled reinforced concrete frames. *Journal of Earthquake Engineering* 2001, Vol.5, No. 1, 1-12.
7. Dolšek M, Fajfar P. Inelastic spectra for infilled reinforced concrete frames. *Earthquake Engineering and structural Dynamics* 2004, Vol.33, 1395-1416.
8. Dolšek M, Fajfar P. Simplfied non-linear seismic analysis of infilled reinforced concrete frames. *Earthquake Engineering and structural Dynamics* 2005, Vol.34, 49-66.
9. Colangelo F. Pseudo-dynamic seismic response of reinforced concrete frames infilled with non-structural brick masonry. *Earthquake Engineering and structural Dynamics* 2005, Vol.34, 1219-1241.
10. Chrysostomou C.Z., Gergely P., Abel J.F. A six-strut model for nonlinear dynamic analysis of steel infilled frames. *International Journal of Structural Stability and Dynamics* 2002, Vol. 2, 335-353.
11. El-Dakhakhni W.W., Elgaaly M., Hamid A.A: Three-strut model for concrete masonry-infilled steel frames. *Journal of Structural Engineering* 2003 February 177-185
12. Crisafulli F.J., 1997. Seismic behaviour of reinforced concrete structures with masonry infills (Ph.D. Thesis). University of Canterbury. Christchurch, New Zealand.
13. CS.LL.PP.; 2009: Istruzioni per l'applicazione delle norme tecniche delle costruzioni. Gazzetta Ufficiale della Repubblica Italiana, 47.

14. Comitè Europèen de Normalisation, 2005. Eurocode8, Design of Structures for earthquake resistance – Part3: Assessment and retrofitting of buildings. EN 1998-1, CEN, Brussels.
15. Paulay T. and Priestley M.J.N. Seismic Design of Reinforced Concrete Structures and Masonry Buildings. Wiley, New York, 1992.
16. Verderame G.M., Iervolino I., Ricci P., 2009. Report on the damages on buildings following the seismic event of 6th of April 2009, V1.20. http://www.reluis.it/.
17. Decreto Ministeriale n. 40 del 3/3/1975, "Approvazione delle norme tecniche per le costruzioni in zone sismiche", G.U. n. 93 dell'8/4/1975.
18. Verderame G.M., Polese M., Mariniello C, Manfredi G. A simulated design procedure for the assessment of seismic capacity of existing reinforced concrete buildings. *Advances in Engineering Software* 2009. doi:10.1016/j.advengsoft.2009.06.011 (in press)
19. Fardis M.N., 1997. Experimental and numerical investigations on the seismic response of RC infilled frames and recommendations for code provisions. Report ECOEST-PREC8 No 6. Prenormative research in support of Eurocode 8.
20. Computers and Structures (2007), SAP 2000. Linear and nonlinear static and dynamic analysis and design of three dimensional structures. CSi, Berkeley, California.
21. Ellul F., D'Ayala D., 2008. Push-over non linear analysis of infilled frames: realistic f e models of panels and contact. Proceedings of The 14th World Conference on Earthquake Engineering, October 12-17, Beijing, China.
22. Buonopane S.G., White R.N., 1999. Pseudodynamic testing of masonry-infilled reinforced concrete frame. Journal of Structural Engineering, Vol. 125, Issue 6, pp. 578-589.
23. Mosalam K., White R.N., Gergely P., 1997. Seismic evaluation of frames with infill walls using pseudodynamic experiments. Rep. No. NCEER-97-0020.
24. Kaushik H.B., Rai D.C., Jain S.K., 2008. A rational approach to analytical modeling of masonry infills in reinforced concrete frame buildings. Proceedings of The 14th World Conference on Earthquake Engineering, October 12-17, Beijing, China.
25. Mainstone R.J., 1971. On the stiffnesses and strengths of infilled frames, Proceedings of the Institution of Civil Engineering, Supplement IV, 57-90.
26. Park R., Paulay T. Reinforced Concrete Structures. Wiley, New York, 1975.
27. Paulay T., Priestley M.J.N. Seismic Design of Reinforced Concrete Structures and Masonry Buildings. Wiley, New York, 1992.
28. Birkeland, P. W., and Birkeland, H. W. Connections in Precast Concrete Construction. *ACI Journal, Proceedings* 63(3), Mar. 1966, 345-368.
29. ACI 318-05. Building code requirements for structural concrete (ACI 318-05) and commentary (ACI 318R-05). ACI committee 318 structural building code. American Concrete Institute, 2005
30. Hofbeck J.A., Ibrahim I.O. and Mattock A.H. Shear transfer in reinforced concrete. *ACI Journal* 66(13), February 1969, 119-128.
31. Ameri G., Augliera P., Bindi D., D'Alema E., Ladina C., Lovati S., Luzi L., Marzorati S., Massa M., Pacor F. and Puglia R. Strong-Motion parameters of the M_w = 6.3 Abruzzo (Central Italy) Earthquake. 2009, http://esse4.mi.ingv.it/.
32. Chioccarelli E., De Luca F., Iervolino I. Preliminary study on L'Aquila earthquake ground motion records V5.20. 2009, http://www.reluis.it/.
33. Bommer J.J, Acevedo A.B. The use of real earthquake accelerograms as input to dynamic analysis. *Journal of Earthquake Engineering* 2004, 8 (Special Issue I), 43-91.
34. CS.LL.PP; DM 14 Gennaio 2008 Allegato A alle Norme Tecniche per le Costruzioni: Pericolosità Sismica. Gazzetta Ufficiale della Repubblica Italiana, 29.
35. Chioccarelli E., Iervolino I., 2010. Near-source seismic demand and pulse-like records: A discussion for L'Aquila earthquake. Earthquake Engineering and Structural Dynamics, Volume 39, Issue 9, Pp. 1039-1062.